

# A FOKKER-PLANCK FRAMEWORK FOR CONTROL OF EPIDEMICS

CHRISTIAN PARKINSON AND SOUVIK ROY

**ABSTRACT.** We present a control framework for stochastic compartmental models in epidemiology. In this framework, rather than directly controlling the stochastic system, we perform optimal control of an associated Fokker-Planck equation, with the goal of steering the distribution of possible solutions of the stochastic system to some desirable state. In particular, this allows for robust control mechanism with uncertainty not only in the dynamics, but also in the initial data. We formulate and fully analyze a partial differential equation constrained optimization problem, including a proof of existence of optimal controls via analysis of the control-to-state map, and a characterization of optimal controls via the Pontryagin minimum principle. We describe the application of the sequential quadratic Hamiltonian method to our problem, which provides numerical approximations of optimal control maps. We demonstrate our method using a minimal stochastic susceptible-infected-recovered model with different choices of cost functionals that represent different policy-maker concerns.

## 1. INTRODUCTION

Since the COVID-19 pandemic, optimal public policy for the control of infectious disease spread has become a problem of acute interest. In this manuscript, we propose a novel framework for control of compartmental epidemiological models based on a partial differential equation (PDE) constrained optimization problem involving the Fokker-Planck equation associated with a stochastic differential equation modeling spread of a generic infectious disease.

Several authors studied general optimal control of basic epidemiological models even before the onset of the COVID-19 pandemic [6, 7, 61], and since the pandemic, there have been more targeted studies regarding various facets of epidemic control such as quarantine implementation [17, 23, 50], vaccination strategies [30, 32, 39], spatial heterogeneity [9, 16, 25], and human behavioral effects [28, 36, 37]. Several of these resources consider control of systems involving stochastic effects, but since they rely on classical results such as the (stochastic) Pontryagin maximum principle [22, Ch. 2.5], [60, Ch. 3.3], they require deterministic initial data.

Parallel to this work in optimal control of epidemic models, there has been theoretical development of so-called Liouville [14] or Fokker-Planck [1, 12] control frameworks, wherein one controls a system of deterministic or stochastic differential equations with uncertain initial data, with the goal of achieving a desirable distribution of possible states at some future time. Among other applications, these have been successfully used in models of collective motion for both pedestrians [10, 42, 43] and traffic flow [41], object identification in image analysis [4], and optimal medical treatment [20, 45, 48].

This work serves to fill a gap in the literature. As noted above, the Fokker-Planck control formulation has been successfully used in models from biology and the applied sciences, but as yet, has not been applied to mathematical epidemiology. We contend that the framework is particularly apt for mathematical epidemiology for a few reasons. First, uncertainty in the total infection size is virtually guaranteed in the early stages of an epidemic, and this framework allows for uncertain initial data in contrast to any framework based on classical methods such as dynamic programming or direct application of the Pontryagin minimum principle to the stochastic system. Second, this framework provides robust control strategies which consider the whole distribution of possible

---

*Date:* January 29, 2026.

solutions to the system of stochastic differential equations that describe disease spread, rather than optimizing for an individual trajectory. This is especially advantageous in the presence of  $L^1$  control costs where the optimal control strategy is often bang-bang (see [33, Ch. 17] or [47, 56]), meaning that nearby trajectories may have significantly different optimal controls. For such systems, direct open loop control of the stochastic system is precarious because random perturbations may push the system to nearby states where the open loop controller provides severely suboptimal control actions. Third, control of the distribution of possible trajectories provides natural answers to probabilistic questions that may be of interest for policy-makers. For example, assuming a certain stochastic model, suppose a policy-maker wants to know whether a given control strategy will result a 50% likelihood of disease extinction by a given future time. This question is more difficult to answer if one considers control of individual trajectories, but very easy to answer if one controls the distribution of all possible trajectories. Thus, to close this gap in the literature, we describe and analyze a simple open loop Fokker-Planck control framework applied to a minimal stochastic model for epidemiology, though with small tweaks, this framework can be applied much more broadly.

Besides formulation and analysis of the Fokker-Planck control framework for epidemiology, we also introduce the sequential quadratic Hamiltonian (SQH) method [11] to the the epidemiology literature for the first time (to the authors' knowledge). This is a numerical method for approximating optimal control maps which is equipped with a much more robust theoretical framework than some other popular methods such as the forward-backward sweep method used by [61, 39, 23, 28] among many others. The SQH method is relatively easy to implement and is completely explainable, in contrast to popular software packages such as the freely available IPOPT<sup>1</sup> [57], as used by [17, 32], which is very robust and explainable to experts in optimization, but is often effectively a black box to practitioner.

The remainder of the manuscript is structured as follows. In section 2, we introduce a simple controlled stochastic susceptible-infected-recovered (SIR) model, make some remarks about the associated controlled Fokker-Planck equation, and formulate an optimal control problem. In section 3, we prove existence of optimal control maps for our problem via analysis of the control-to-state map and derive first-order optimality conditions which characterize the optimal controls. In section 4, we discuss the numerical methods we use to computationally approximate the optimal controls, and in particular, give an exposition of the SQH method [11] as it pertains to our problem. In section 5, we present results of the application of our method to control problems involving our model wherein costs are accumulated in different manners representing different potential concerns of policy-makers. Finally, we give some concluding remarks and discuss avenues of future work in section 6.

## 2. A CONTROLLED STOCHASTIC SIR MODEL AND FOKKER-PLANCK EQUATION

We begin from the basic SIR model of Kermack and McKendrick [29], which models infectious disease spread through a homogeneous population which is split into susceptible, infected, and recovered subpopulations. We assume a natural birth rate  $b$ , natural death rate  $\delta$ , infection rate  $\beta$  and recovery rate  $\gamma$ , and we add three controls which may be available to a real-world policy-maker: (1) a reduction in infectivity of the disease due to the implementation of non-pharmaceutical intervention (NPI) measures such as mask-wearing, shelter-at-home, or social-distancing mandates; (2) vaccination efforts which move susceptible individuals directly to the recovered class without passing through the infected class; (3) increase in recovery rate due to treatment efforts. Representing

---

<sup>1</sup><https://github.com/coin-or/Ipopt>

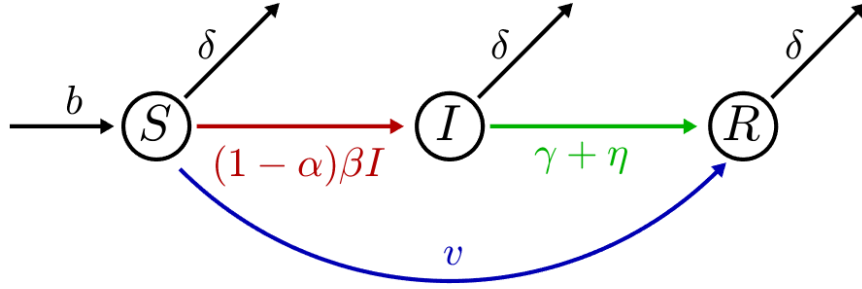


**Figure 1.** The flow diagram for (1) in the absence of noise. Colored lines represent our modifications to the basic SIR model; these are the terms where the control variables  $\alpha, \eta, v$  appear.

these controls (respectively) by  $\alpha \in [0, \alpha_{\max}], v \in [0, v_{\max}], \eta \in [0, \eta_{\max}]$ , this leads to the model

$$(1) \quad \begin{aligned} \dot{S} &= b - (1 - \alpha(t))\beta SI - (v(t) + \delta)S, \\ \dot{I} &= (1 - \alpha(t))\beta SI - (\gamma + \eta(t) + \delta)I, \\ \dot{R} &= (\gamma + \eta(t))I + v(t)S - \delta R, \end{aligned}$$

along with nonnegative initial conditions  $S(0) = S_0, I(0) = I_0, R(0) = R_0$ . The flow diagram for this model is included in figure 1, where any arrows flowing out of a compartment denote flow proportional to the compartment they are leaving. In particular, the colored arrows in the diagram represent our modifications to the basic SIR model. These are the terms where the control variables appear.

We add stochasticity into the model in two ways. First, we treat the initial data as uncertain, so that rather than being specified exactly, we assume  $S_0, I_0, R_0$  are drawn from a specified probability distribution. And second, we perturb each equation in (1) with an Itô noise term with respective strengths  $\sigma_S, \sigma_I, \sigma_R$ . In the epidemiological literature, common choices for these stochastic terms are to either let the noise in each equation be proportional to the population which the equation describes [27, 59, 62], or to more explicitly model uncertainty in disease transmission by taking  $\sigma_I = -\sigma_S \propto SI$  which is equivalent to formally replacing  $\beta$  with  $\beta + \sigma_\beta \dot{W}$  where  $W$  is Itô white noise [24, 26, 38, 54]. In the Fokker-Planck control literature, it is relatively common to let these terms be constant for ease of analysis; for example [12, 43]. In any of these cases,  $\sigma_S$  and  $\sigma_I$  are independent of  $R$ , which means that  $\dot{S}$  and  $\dot{I}$  are entirely independent of  $R$ , at which point the  $R$  compartment is simply a receptacle for those who are vaccinated or recovered, and has no bearing on disease spread dynamics. In accordance with this observation and in order to simplify the model, we will always make the assumption that  $\sigma_S, \sigma_I$  are independent of  $R$ , whereupon we focus of the following system of two stochastic differential equations describing infectious disease spread:

$$(2) \quad \begin{aligned} dS &= \left( b - (1 - \alpha)\beta SI - (v(t) + \delta)S \right) dt + \sigma_S(S, I, \alpha, \eta, v) dW_1, \\ dI &= \left( (1 - \alpha)\beta SI - (\gamma + \eta(t) + \delta)I \right) dt + \sigma_I(S, I, \alpha, \eta, v) dW_2 \end{aligned}$$

where  $W_1, W_2$  are the (stochastically independent) components of a 2-dimensional Weiner process.

For more compact notation, we can define  $X = (X_1, X_2) := (S, I)$  and  $u = (u_1, u_2, u_3) := (\alpha, v, \eta)$ , and write (2) as

$$(3) \quad dX = \mathbf{F}(X, u) dt + \boldsymbol{\sigma}(X, u) d\mathbf{W}$$

where

$$(4) \quad \mathbf{F}(x, u) = \begin{bmatrix} b - (1 - u_1)\beta x_1 x_2 - (u_2 + \delta)x_1, \\ (1 - u_1)\beta x_1 x_2 - (\gamma + u_3 + \delta)x_2. \end{bmatrix}$$

and

$$(5) \quad \boldsymbol{\sigma}(x, u) = \begin{bmatrix} \sigma_1(x, u) & 0 \\ 0 & \sigma_2(x, u) \end{bmatrix} = \begin{bmatrix} \sigma_S(S, I, \alpha, \eta, v) & 0 \\ 0 & \sigma_I(S, I, \alpha, \eta, v) \end{bmatrix},$$

and  $\mathbf{W}$  is a 2-dimensional Weiner process with stochastically independent components.

We assume the existence of a bounded domain  $\Omega \subset \mathbb{R}^2$  with Lipschitz boundary which is positively invariant under the dynamics (3), whereupon we consider initial data  $X_0$  drawn from a probability distribution with density function  $f_0(x)$  defined on  $\Omega$ . Note that existence of such  $\Omega$  is not a prohibitive assumption. So long as the functions  $\sigma_S, \sigma_I, \frac{\sigma_S}{S}, \frac{\sigma_I}{I}$  are bounded for bounded values of their inputs (which is true, for example, when  $\sigma_S, \sigma_I$  are continuous and proportional to  $S, I$  respectively), global existence of a bounded, nonnegative solution of (3) follows directly as in [24, 26, 27, 62], whereupon one can take  $\Omega = (a_{\min}, a_{\max})^2$  for any  $a_{\min} \leq 0$  and  $a_{\max} > 0$  sufficiently large. Besides this, for the sake of theoretical results below, we will always assume that  $\sigma_S^2, \sigma_I^2$  are twice continuously differentiable in  $x$ , and continuous in  $u$ .

Given this the Fokker-Planck equation describing the evolution of the probability distribution function for the solution of (3) is given by

$$(6) \quad \partial_t f(x, t) + \nabla \cdot (\mathbf{F}(x, u) f(x, t)) = \frac{1}{2} \sum_{j=1}^2 \frac{\partial^2}{\partial x_j^2} (\sigma_j^2(x, u) f(x, t)), \quad \text{in } \Omega \times (0, T],$$

$$f(x, 0) = f_0(x), \quad \text{in } \Omega,$$

along with zero flux boundary conditions  $\mathcal{F} \cdot \hat{n} = 0$  on  $\partial\Omega \times (0, T]$ , where  $\mathcal{F}$  is the flux, defined componentwise by

$$(7) \quad \mathcal{F}_j(x, t) = \frac{1}{2} \frac{\partial}{\partial x_j} \left( \sigma_j(x, t)^2 f(x, t) \right) - \mathbf{F}_j(x, u) f(x, t), \quad j = 1, 2.$$

For a derivation of the Fokker-Planck equation and discussion of related topics, see [40]. The time horizon  $T > 0$  in (6) is somewhat artificial. In theory, the time interval  $(0, T)$  could be replaced with  $(0, \infty)$ . However, for the sake of formulating an optimal control problem, we will consider the finite time interval.

Note that (6) can be written in divergence form in which case, dropping arguments for brevity, the equation reads

$$(8) \quad \partial_t f + \sum_{j=1}^2 \left( b_j \frac{\partial f}{\partial x_j} \right) + c f = \frac{1}{2} \sum_{j=1}^2 \frac{\partial}{\partial x_j} \left( \sigma_j^2 \frac{\partial f}{\partial x_j} \right)$$

where  $b_j = F_j - \frac{\partial}{\partial x_j} \sigma_j^2$  and  $c = \frac{\partial b_1}{\partial x_1} + \frac{\partial b_2}{\partial x_2}$ . This formulation is amenable to the definition of weak solutions as described in [21, Ch. 7.1], [58, Ch. 3.5]. Formally, we say that  $f$  is a weak solution of (6) if

$$(9) \quad \int_0^T \int_{\Omega} \left( f_t \varphi + \frac{1}{2} \sum_{j=1}^2 b_j \frac{\partial f}{\partial x_j} \varphi + c f \varphi \right) dx dt = 0, \quad \text{for all } \varphi \in C^1(Q) \text{ with } \nabla \varphi \cdot \hat{n} = 0.$$

Since  $\mathbf{F}(x, u)$  is a smooth function of  $x$  and remains bounded so long as  $u$  is bounded and  $\sigma_S, \sigma_I$  are twice continuously differentiable in  $x$ , and continuous in  $u$ , the  $b_j$  and  $c$  are continuous (and thus bounded for  $x \in \Omega$  and bounded choice of controls). Thus the following proposition regarding existence and uniqueness of a weak solution of (6) follows from [58, Ch. 3, Theorem 3.5.1], [31, Ch. IV, Theorem 9.1].

**Proposition 2.1.** *For fixed bounded control map  $u : [0, T] \rightarrow \mathbb{R}^3$  and  $f_0 \in H^1(\Omega)$ , there exists a unique weak solution  $f \in H^{2,1}(Q)$  of (6). Moreover, if  $f_0 \geq 0$  in  $\Omega$  and  $\|f_0\|_{L^1(\Omega)} = 1$ , then  $f \geq 0$  in  $Q$  and  $\|f(\cdot, t)\|_{L^1(\Omega)} = 1$  for all  $t \in (0, T]$ .*

**Remark 2.1.** The result from [58, Ch. 3, Theorem 3.5.1] only guarantees a solution  $f \in H^{1,1}(Q)$  when  $f_0 \in L^2(\Omega)$ , but presents a more tightly contained discussion of the weak formulation and related principles. The result from [31, Ch. IV, Theorem 9.1] guarantees existence of a unique solution  $f \in H^{2,1}(\Omega)$  of (6) when  $f_0 \in H^1(\Omega)$  using different methods, and importantly includes a bound on  $\|f\|_{H^{2,1}(Q)}$  which is uniform over choices of controls  $u$  that are uniformly bounded in  $(L^\infty[0, T])^3$ , a property we use below. Of course, the uniqueness guarantees that these two solutions agree when we assume the more stringent conditions. The mass and positivity preservation follow from classical analysis of the equation, not directly from these regularity results.

Given this, we consider controls taking values in the rectangle  $R_U = [0, \alpha_{\max}] \times [0, v_{\max}] \times [0, \eta_{\max}]$ , so that the admissible control space is

$$(10) \quad U_{\text{ad}} := \left\{ u : [0, T] \rightarrow \mathbb{R}^3 \mid u \text{ is measurable and } u(t) \in R_U \text{ for a.e. } t \in [0, T] \right\} \subset (L^\infty[0, T])^3.$$

In a slight abuse of vocabulary, for a given  $u \in U_{\text{ad}}$ , we will often refer to the function  $f \in H^{2,1}(Q)$  guaranteed by proposition 2.1 as the solution of (6) corresponding to  $u$ , brushing over the fact that we are considering a weak solution as defined above.

Our optimal control problem for (6) is then stated abstractly as

$$(11) \quad \min_{f,u} J(f, u) := \int_0^T \ell(u(t)) dt + \int_{\Omega} K(x) f(x, T) dx + \int_0^T \int_{\Omega} G(x, t) f(x, t) dx dt \\ \text{such that } u \in U_{\text{ad}} \text{ and } f \text{ satisfies (6),}$$

where  $K(x)$  assesses cost based on the final distribution  $f(x, T)$ ,  $G(x, t)$  assesses running cost throughout the time interval, and  $\ell(u) \geq 0$  assesses control costs. That  $J(f, u)$  is bounded below follows, as long as  $K$  and  $G$  are bounded, from the nonnegativity and  $L^1$  boundedness of  $f$ , which is uniform over choices of  $u \in U_{\text{ad}}$ . Because of this, we will, at a minimum, assume that  $K, G$  are bounded on their domains, and specify some further constraints as needed below.

### 3. ANALYSIS OF THE FOKKER-PLANCK CONTROL PROBLEM

In this section, we provide some analysis of the Fokker-Planck control problem (11). Specifically, we give necessary conditions which characterize the optimal control maps via a version of the Pontryagin Minimum Principle (PMP) in the vein of [12]. Before doing so, we prove existence of an optimal control by analyzing the control-to-state map.

**Theorem 3.1.** *Assume that the control cost  $\ell : R_U \rightarrow [0, \infty)$  is continuous and convex, and that  $\sigma_S^2, \sigma_I^2$  are twice differentiable in  $x$  and Lipschitz continuous in  $u$  with a Lipschitz constant which is uniform over  $x \in \Omega$ . Then there exists an optimal control  $u^* \in U_{\text{ad}}$  and corresponding solution  $f^*$  of (6) which solve (11).*

*Proof.* The proof follows the general strategy of [3, Corollary 1], which entails analysis of the control-to-state map. Here the control-to-state map

$$(12) \quad u \in U_{\text{ad}} \subset (L^2[0, T])^3 \mapsto \mathcal{S}(u) = f \in H^{2,1}(Q) \subset H^{1,1}(Q), \text{ the solution of (6)}$$

is well-defined by virtue of proposition 2.1. Note, we are considering  $U_{\text{ad}}$  with the norm

$$\|u\|_{(L^2[0, T])^3} = \left( \sum_{i=1}^3 \|u_i\|_{L^2[0, T]}^2 \right)^{1/2}.$$

As a closed subset of a Hilbert space,  $U_{\text{ad}}$  is itself a Hilbert space. We prove the following two properties:

- (a)  $\mathcal{S}$  is weakly closed as a map from  $U_{\text{ad}} \rightarrow L^2(Q)$ . That is, if a sequence  $\{u^{(k)}\}$  in  $U_{\text{ad}}$  is such that  $u^{(k)} \rightharpoonup u$  in  $(L^2[0, T])^3$  and  $\mathcal{S}(u^{(k)}) \rightharpoonup f \in L^2(Q)$ , then  $u \in U_{\text{ad}}$  and  $\mathcal{S}(u) = f$ .

(b)  $\mathcal{S}$  is weak-strong continuous as a map from  $U_{\text{ad}} \rightarrow L^2(Q)$ .

For (a), take a sequence  $\{u^{(k)}\}$  in  $U_{\text{ad}}$  such that  $u^{(k)} \rightharpoonup u$  in  $(L^2[0, T])^3$  and  $\mathcal{S}(u^{(k)}) \rightharpoonup f \in L^2(Q)$ . That  $u \in U_{\text{ad}}$  follows because  $U_{\text{ad}}$  is both strongly closed and convex, and hence weakly closed [13, Ch. 3.3]. Now  $\{\mathcal{S}(u^{(k)})\}$  is a bounded sequence in the Hilbert space  $H^{1,1}(Q)$  and hence has a subsequence weakly converging to some  $f_1 \in H^{1,1}(Q)$ . By compactness of the embedding  $H^{1,1}(Q) \hookrightarrow L^2(Q)$  [34, Ch. 12], passing to a further subsequence if necessary,  $\mathcal{S}(u^{(k)})$  must converge strongly to  $f_1$  in the  $L^2(Q)$  topology (and thus also weakly). By uniqueness of limits, this implies  $f_1 = f$ . By the uniform  $L^\infty$  bounds on the coefficients  $b_j, c$  in (9), weak convergence of  $u^{(k)} \rightarrow u$  in  $L^2[0, T]$ , weak convergence of  $\mathcal{S}(u^{(k)})$  to  $f$  in  $H^{1,1}(Q)$ , and strong convergence of  $\mathcal{S}(u^{(k)})$  to  $f$  in  $L^2(Q)$ , we see from (9), that  $f$  must be a weak solution of (6) corresponding to the control  $u \in U_{\text{ad}}$ . By definition,  $\mathcal{S}(u)$  is the unique such weak solution, so  $\mathcal{S}(u) = f$ . This concludes the proof of (a).

For (b), we use a simple application of the Urysohn subsequence principle [52, Ch. 2.1.17]. Suppose that  $\{u^{(k)}\}$  is a sequence converging weakly to  $u \in U_{\text{ad}}$ . Again  $\{\mathcal{S}(u^{(k)})\}$  is a uniformly bounded sequence in  $H^{1,1}(Q)$ . Thus any subsequence  $\{\mathcal{S}(u^{(k_\ell)})\}$  is uniformly bounded in  $H^{1,1}(Q)$ , and thus once again by the compact embedding  $H^{1,1}(Q) \hookrightarrow L^2(Q)$ , there is a further subsequence  $\{\mathcal{S}(u^{k_{\ell_m}})\}$  converging strongly to some  $f \in L^2(Q)$ . By the closure guaranteed in (a), we must have  $\mathcal{S}(u) = f$ . Thus every subsequence of  $\{\mathcal{S}(u^{(k)})\}$  has a further subsequence converging strongly to  $\mathcal{S}(u)$ , so Urysohn's principle implies that  $\mathcal{S}(u_n) \rightarrow \mathcal{S}(u)$  and  $\mathcal{S}$  is weak-strong continuous from  $U_{\text{ad}} \rightarrow L^2(Q)$ .

Finally, consider the reduced cost functional  $\mathcal{J}(u) = J(\mathcal{S}(u), u)$ . Since the control-to-state operator is well-defined, problem (11) is equivalent to

$$(13) \quad \min_{u \in U_{\text{ad}}} \mathcal{J}(u)$$

Now  $\mathcal{J}(u)$  is bounded from below so  $\inf_{u \in U_{\text{ad}}} \mathcal{J}(u) = J^*$  is finite. Take a minimizing sequence  $\{u^{(k)}\}$  such that  $\mathcal{J}(u^{(k)}) \rightarrow J^*$ . Since  $\{u^{(k)}\}$  is a bounded sequence in  $(L^2[0, T])^3$ , we can pass to a subsequence which converges weakly to some  $u^* \in U_{\text{ad}}$ , and by weak-strong continuity proven in (b), we know that  $\mathcal{S}(u^{(k)}) \rightarrow \mathcal{S}(u)$  strongly in  $L^2(Q)$  along this subsequence. Now,

$$\mathcal{J}(u^{(k)}) = \int_0^T \ell(u^{(k)}(t)) dt + \int_{\Omega} K(x)[\mathcal{S}(u^{(k)})](x, T) dt + \int_0^T \int_{\Omega} G(x, t)[\mathcal{S}(u^{(k)})](x, t) dx dt.$$

The conditions that  $\ell$  is nonnegative, continuous and convex guarantee that the first term above is weakly lower-semicontinuous in  $u$ . The weak-strong continuity of  $\mathcal{S}(u)$  guarantees that the latter two terms are well-behaved in the limit as  $k \rightarrow \infty$  since  $K, G$  are bounded. Thus we see

$$J^* \leq \mathcal{J}(u^*) \leq \liminf_{k \rightarrow \infty} \mathcal{J}(u^{(k)}) = J^*,$$

so indeed this  $u^* \in U_{\text{ad}}$  and the corresponding  $f^* := \mathcal{S}(u^*) \in H^{2,1}(Q)$  are a solution of (11).  $\square$

We remark that we also have strong-strong continuity of the control-to-state map. While this is not enough to conclude existence of a solution to the optimal control problem, it does have bearing on the convergence of the numerical methods, so we briefly derive it here.

**Lemma 3.1.** *The control to state map  $\mathcal{S} : U_{\text{ad}} \rightarrow H^{2,1}(\Omega)$  is strong-strong continuous.*

*Proof.* For controls  $u, \bar{u} \in U_{\text{ad}}$ , we see that  $z = \mathcal{S}(u) - \mathcal{S}(\bar{u}) = f - \bar{f}$  satisfies the equation

$$(14) \quad \partial_t z + \nabla \cdot (\mathbf{F}(x, u)z) - \frac{1}{2} \sum_{j=1}^2 \frac{\partial^2}{\partial x_j^2} (\sigma_j(x, u)z) = \Phi(x, u, \bar{u}, t)$$

where

$$\Phi(x, u, \bar{u}, t) = \nabla \cdot \left( (\mathbf{F}(x, \bar{u}) - \mathbf{F}(x, u)) \bar{f}(x, t) \right) - \frac{1}{2} \sum_{j=1}^2 \frac{\partial^2}{\partial x_j^2} \left( (\sigma_j(x, \bar{u})^2 - \sigma_j(x, u)^2) \bar{f}(x, t) \right),$$

along with  $z(\cdot, 0) = 0$  and a zero flux boundary condition. Since we have assumed that  $\sigma_j(x, u)^2$  is Lipschitz in  $u$ , using that  $\mathbf{F}(x, u)$  is affine in  $u$  and that  $\|\bar{f}\|_{H^{2,1}(Q)}$  is uniformly bounded over choices of  $\bar{u} \in U_{\text{ad}}$ , we see

$$\|\Phi(x, u, \bar{u}, t)\|_{L^2(Q)} \leq C\|u - \bar{u}\|_{(L^2[0,T])^3}.$$

Then from classical parabolic estimates [58, Ch. 9], we have that

$$(15) \quad \|\mathcal{S}(u) - \mathcal{S}(\bar{u})\|_{H^{2,1}(Q)} = \|z\|_{H^{2,1}(Q)} \leq C\|u - \bar{u}\|_{(L^2[0,T])^3},$$

demonstrating that control-to-state map is strong-strong continuous from  $U_{\text{ad}} \rightarrow H^{2,1}(Q)$  when  $U_{\text{ad}}$  has the  $L^2$  topology (in fact it is Lipschitz continuous).  $\square$

In order to characterize this optimal pair, for functions  $f, q : Q \rightarrow \mathbb{R}$  and controls  $u \in U_{\text{ad}}$ , we formally define the Lagrangian for our problem as

$$(16) \quad L(f, q, u) = J(f, u) + \int_0^T \int_{\Omega} q \left( \partial_t f + \nabla \cdot (\mathbf{F}(x, u) f) - \frac{1}{2} \sum_{j=1}^2 \frac{\partial^2}{\partial x_j^2} (\sigma_j(x, u)^2 f) \right) dx dt$$

where we have suppressed the dependence of  $f, q$  on  $(x, t)$  and the dependence of  $u$  on  $t$  for brevity.

Writing out  $J(f, u)$  and integrating by parts, we see

$$(17) \quad \begin{aligned} L(f, q, u) = & \int_0^T \left( \ell(u) + \int_{\Omega} f \left( -\partial_t q - \mathbf{F}(x, u) \cdot \nabla q - \frac{1}{2} \sum_{j=1}^2 \sigma_j(x, u)^2 \frac{\partial^2 q}{\partial x_j^2} + G(x, t) \right) dx \right) \\ & \int_{\Omega} [K(x) + q(x, T)] f(x, T) - f_0(x) q(x, 0) dx. \end{aligned}$$

This motivates the definition of the adjoint equation of (6) for our problem:

$$(18) \quad \begin{aligned} -\partial_t q(x, t) - \mathbf{F}(x, u) \cdot \nabla q(x, t) - \frac{1}{2} \sum_{j=1}^2 \sigma_j^2(x, u) \frac{\partial^2 q}{\partial x_j^2}(x, t) + G(x, t) &= 0, \quad \text{in } \Omega \times (0, T) \\ q(x, T) &= -K(x), \quad \text{in } \Omega, \end{aligned}$$

along with a zero flux boundary condition  $\nabla q \cdot \hat{n} = 0$  on  $\partial\Omega \times (0, T)$ .

Again, existence, uniqueness and some regularity for (18) follows from [31, Ch. IV, Theorem 9.1] given some mild assumptions on  $G(x, t), K(x)$  (in addition to the assumptions we have already imposed on  $\sigma_S, \sigma_I$ ).

**Proposition 3.1.** *Assume that  $K \in H^1(\Omega)$  and  $G \in L^2(Q)$ . Then for a fixed control map  $u \in U_{\text{ad}}$ , there exists a unique solution  $q \in H^{2,1}(Q)$  of (18).*

Using similar formality as with the Lagrangian (16), we now define the Pontryagin Hamiltonian function

$$(19) \quad H(t, f(\cdot, t), q(\cdot, t), u(t)) = \ell(u(t)) - \int_{\Omega} \left( f(\cdot, t) \mathbf{F}(x, u(t)) \cdot \nabla q(\cdot, t) + \frac{1}{2} \sum_{j=1}^2 f(\cdot, t) \sigma_j(\cdot, u(t))^2 \frac{\partial^2 q}{\partial x_j^2}(\cdot, t) \right) dx$$

for  $f, q : Q \rightarrow \mathbb{R}$  and  $u \in U_{\text{ad}}$ . Here we have suppressed the dependence of  $f, q$  on  $x$  but maintain the dependence on  $t$  to emphasize that this Hamiltonian does depend on time.

We want to prove that the optimal controls can be characterized as a pointwise (in time) minimizer of this Hamiltonian, rather than in terms of a variational inequality which is typical for general controlled partial differential equations; see [35, Ch. 9], [55, Ch. 5]. To this end, we prove a lemma expressing the difference of the cost functional evaluated on different controls explicitly in terms of the Hamiltonian (19).

**Lemma 3.2.** *For any two control maps  $u, \bar{u} \in U_{ad}$  with respective solutions  $f$  and  $\bar{f}$  of (6), we have*

$$J(f, u) - J(\bar{f}, \bar{u}) = \int_0^T \left[ H(t, \bar{f}(\cdot, t), q(\cdot, t), u(t)) - H(t, \bar{f}(\cdot, t), q(\cdot, t), \bar{u}(t)) \right] dt$$

where  $q$  is the solution of (18) corresponding to control  $u$ .

*Proof.* Again, we suppress dependence on  $(x, t)$  in the functions  $f, \bar{f}, q$  for brevity, and compute (20)

$$\begin{aligned} J(f, u) - J(\bar{f}, \bar{u}) &= \int_0^T [\ell(u(t)) - \ell(\bar{u}(t))] dt + \int_{\Omega} K(x)[f - \bar{f}](\cdot, T) dx + \int_0^T \int_{\Omega} G(x)[f - \bar{f}] dx dt \\ &= \int_0^T [\ell(u(t)) - \ell(\bar{u}(t))] dt + \int_{\Omega} K(x)[f - \bar{f}](\cdot, T) dx \\ &\quad + \int_0^T \int_{\Omega} \left( \partial_t q + \mathbf{F}(x, u) \cdot \nabla q + \frac{1}{2} \sum_{j=1}^2 \sigma_j(x, u)^2 \frac{\partial^2 q}{\partial x_j^2} \right) [f - \bar{f}] dx dt \\ &= \int_0^T [\ell(u(t)) - \ell(\bar{u}(t))] dt \\ &\quad + \int_0^T \int_{\Omega} \left( -[\partial_t f - \partial_t \bar{f}] - \nabla \cdot (\mathbf{F}(x, u)[f - \bar{f}]) \right) q dx dt \\ &\quad + \int_0^T \int_{\Omega} \frac{1}{2} \sum_{j=1}^2 \frac{\partial^2}{\partial x_j^2} \left( \sigma_j(x, u)^2 [f - \bar{f}] \right) q dx dt, \end{aligned}$$

where, in the last line, we have integrated by parts and canceled boundary terms. Now since  $f$  satisfies (6) with control  $u$ , we see that all terms with  $f$  vanish. Likewise, we replace  $\partial_t \bar{f}$  using (6) with control  $\bar{u}$ . Doing so, we see

$$\begin{aligned} (21) \quad J(f, u) - J(\bar{f}, \bar{u}) &= \int_0^T [\ell(u(t)) - \ell(\bar{u}(t))] dt \\ &\quad + \int_0^T \int_{\Omega} \nabla \cdot ([\mathbf{F}(x, u) - \mathbf{F}(x, \bar{u})] \bar{f}) q dx dt \\ &\quad - \int_0^T \int_{\Omega} \frac{1}{2} \sum_{j=1}^2 \frac{\partial^2}{\partial x_j^2} \left( (\sigma_j(x, u)^2 - \sigma_j(x, \bar{u})^2) \bar{f} \right) q dx dt \\ &= \int_0^T \ell(u(t)) - \left( \int_{\Omega} \bar{f} \mathbf{F}(x, u) \cdot \nabla q - \frac{1}{2} \sum_{j=1}^2 \bar{f} \sigma_j(x, u)^2 \frac{\partial^2 q}{\partial x_j^2} dx \right) dx \\ &\quad - \int_0^T \ell(\bar{u}(t)) - \left( \int_{\Omega} \bar{f} \mathbf{F}(x, \bar{u}) \cdot \nabla q - \frac{1}{2} \sum_{j=1}^2 \bar{f} \sigma_j(x, \bar{u})^2 \frac{\partial^2 q}{\partial x_j^2} dx \right) dx \\ &= \int_0^T \left[ H(t, \bar{f}(\cdot, t), q(\cdot, t), u(t)) - H(t, \bar{f}(\cdot, t), q(\cdot, t), \bar{u}(t)) \right] dt \end{aligned}$$

as desired.  $\square$

With this, we prove a version of the PMP for the Fokker-Planck control problem (11).

**Theorem 3.2.** *Let  $(f^*, u^*)$  be a solution of (11), and let  $q^*$  be the solution of the corresponding adjoint equation (18). Then*

$$(22) \quad H(t, f^*(\cdot, t), q^*(\cdot, t), u^*(t)) = \min_{w \in R_U} H(t, f^*(\cdot, t), q^*(\cdot, t), w).$$

for almost all  $t \in [0, T]$ .

*Proof.* The proof uses a so-called needle variation of the optimal control map  $u^* \in U_{\text{ad}}$ . Taking any admissible control action  $w \in R_U$  and any  $t_0 \in [0, T]$ , we let  $B_k(t_0)$  be a sequence of balls centered at  $t_0$  such that  $|B(t_0)| \rightarrow 0$  as  $k \rightarrow \infty$ , and define

$$(23) \quad u_k(t) = \begin{cases} u^*(t), & t \in [0, T] \setminus B_k(t_0), \\ w, & t \in [0, T] \cap B_k(t_0). \end{cases}$$

We let  $f_k$  be the solution of (6) and  $q_k$  be the solution of (18) corresponding to  $u_k$ . Then by lemma 3.2, we see

$$(24) \quad \begin{aligned} 0 \leq \frac{J(f_k, u_k) - J(f^*, u^*)}{|B_k(t_0)|} &= \frac{1}{|B_k(t_0)|} \int_0^T [H(t, f^*, q_k, u_k) - H(t, f^*, q_k, u^*)] dx dt \\ &= \frac{1}{|B_k(t_0)|} \int_{B_k(t_0)} [H(t, f^*, q_k, w) - H(t, f^*, q_k, u^*)] dt \\ &= \frac{1}{|B_k(t_0)|} \int_{B_k(t_0)} [H(t, f^*, q^*, w) - H(t, f^*, q^*, u^*)] dt \\ &\quad + \frac{1}{|B_k(t_0)|} \int_{B_k(t_0)} \int_{\Omega} f^* \mathbf{F}(x, u^*) \cdot \nabla(q_k - q^*) dx dt \\ &\quad + \frac{1}{|B_k(t_0)|} \int_{B_k(t_0)} \int_{\Omega} \frac{1}{2} \sum_{j=1}^2 f^* \sigma_j(x, u^*)^2 \frac{\partial^2}{\partial x_j^2} (q_k - q^*) dx dt \\ &\quad + \frac{1}{|B_k(t_0)|} \int_{B_k(t_0)} \int_{\Omega} f^* \mathbf{F}(x, w) \cdot \nabla(q_k - q^*) dx dt \\ &\quad + \frac{1}{|B_k(t_0)|} \int_{B_k(t_0)} \int_{\Omega} \frac{1}{2} \sum_{j=1}^2 f^* \sigma_j(x, w)^2 \frac{\partial^2}{\partial x_j^2} (q_k - q^*) dx dt. \end{aligned}$$

By the same argument as in [12, §3, Theorem 5], we have that  $\|q_k - q^*\|_{L^\infty(Q)} \rightarrow 0$  as  $k \rightarrow \infty$ , whereupon, after integrating by parts to pass derivatives onto  $f^* \in H^{2,1}(Q)$  and invoking the smoothness of  $\mathbf{F}(x, u)$ ,  $\sigma(x, u)$  as functions of  $x$ , we see that the last four lines of (24) go to zero as  $k \rightarrow \infty$ .

Finally, since  $f^*, q^*$  are sufficiently regular, the map  $t \mapsto [H(t, f^*, q^*, w) - H(t, f^*, q^*, u^*)]$  is in  $L^1[0, T]$  and thus by the Lebesgue differentiation theorem [46, Theorem 7.10], we can take the limit as  $k \rightarrow \infty$  in (24) and conclude that for almost every  $t \in [0, T]$ ,

$$0 \leq H(t, f^*(\cdot, t), q^*(\cdot, t), w) - H(t, f^*(\cdot, t), q^*(\cdot, t), u^*(t)).$$

Since  $w \in R_U$  was arbitrary, this proves (22).  $\square$

Having proven this, we state the full necessary optimality conditions as a corollary.

**Corollary 3.1** (Necessary Conditions for Optimality). *If  $(f, u)$  is a solution of the Fokker-Planck control problem (11), then there exists  $q$  such that the following optimality system holds:*

$$(FP) \quad \begin{cases} \partial_t f(x, t) + \nabla \cdot (\mathbf{F}(x, u) f(x, t)) = \frac{1}{2} \sum_{j=1}^2 \frac{\partial^2}{\partial x_j^2} (\sigma_j^2(x, u) f(x, t)), & \text{in } \Omega \times (0, T], \\ f(x, 0) = f_0(x), & \text{in } \Omega, \quad \mathcal{F} \cdot \hat{n} = 0, \quad \text{on } \partial\Omega \text{ for } \mathcal{F} \text{ as defined in (7),} \end{cases}$$

$$(ADJ) \quad \begin{cases} -\partial_t q(x, t) - \mathbf{F}(x, u) \cdot \nabla q(x, t) = \frac{1}{2} \sum_{j=1}^2 \sigma_j^2(x, u) \frac{\partial^2 q}{\partial x_j^2}(x, t) - G(x, t), & \text{in } \Omega \times (0, T) \\ q(x, T) = -K(x), & \text{in } \Omega, \quad \nabla q \cdot \hat{n} = 0, \quad \text{on } \partial\Omega, \end{cases}$$

$$(PMP) \quad H(t, f(\cdot, t), q(\cdot, t), u(t)) = \min_{w \in R_U} H(t, f(\cdot, t), q(\cdot, t), w).$$

#### 4. COMPUTATIONAL METHODS

In this section, we describe the numerical methods used to solve the FP control problem (11). This includes finite difference schemes for solving the forward and adjoint FP equations, (FP) and (ADJ) respectively, and a brief exposition of the sequential quadratic Hamiltonian (SQH) method for resolving the optimal control maps. A fuller exposition of the SQH method with several examples can be found in [11].

To solve for the forward and adjoint Liouville equations (FP) and (ADJ), we use a strong stability preserving Runge-Kutta time discretization scheme coupled with the Chang-Cooper spatial discretization scheme and also implement a Strang splitting method. The details of the complete scheme can be found in [44, 45].

The sequential quadratic Hamiltonian (SQH) method is an iterative method of resolving the optimal control for (11) by using successive quadratic perturbations, which act as approximations to the true Hamiltonian (19). Pseudocode for the method is detailed in algorithm 1, and we describe it here. For a penalization parameter  $\varepsilon > 0$ , we formally define the quadratically augmented Hamiltonian by

$$(25) \quad H_\varepsilon(t, f(\cdot, t), q(\cdot, t), u(t), \tilde{u}(t)) = H(t, f(\cdot, t), q(\cdot, t), \tilde{u}(t)) + \varepsilon |u(t) - \tilde{u}(t)|_2^2$$

where  $H$  is the Hamiltonian defined in (19),  $f, q$  are functions on  $Q$  and  $u, \tilde{u} \in U_{ad}$ . We will use this augmented Hamiltonian while adaptively adjusting the parameter  $\varepsilon$  at each iteration of the SQH process. Specifically,  $\varepsilon$  is increased if a sufficient decrease in the functional  $J(f, u)$  is not observed, and decreased if  $J(f, u)$  decreases adequately. Here,  $\tilde{u}$  represents the previous approximations of the control  $u$  and the purpose of the quadratic term  $\varepsilon |u - \tilde{u}|_2^2$  is to ensure that the pointwise minimizer of  $H_\varepsilon$ , and thus the updates to  $u$  remain close to the prior values  $\tilde{u}$ , especially when  $\varepsilon$  is large. An important note is that during the iteration, specifically in step (ii), the values of  $f$  and  $q$  used to update  $u$  are those obtained from the previous iteration.

We further note that in step (v) of this algorithm, if the inequality  $J(f^{k+1}, u^{k+1}) - J(f^k, u^k) > -\mu \tau$  holds, this indicates that a sufficient decrease in the objective functional  $J(f, u)$  has not been achieved. In such a case, the setting  $\varepsilon \leftarrow \lambda \varepsilon$  causes an increase in  $\varepsilon$  since  $\lambda > 1$ , and by returning to step (2), we restart the iteration with the updated augmented Hamiltonian function. Conversely, if the inequality does not hold, it confirms that the required reduction in  $J(f, u)$  has been met. The updated control  $u^{k+1}$  is then adopted, along with the corresponding updates  $f^{k+1}$  and  $q^{k+1}$  as the solutions to (FP) and (ADJ) respectively. In this situation,  $\varepsilon \leftarrow \zeta \varepsilon$  causes a reduction in  $\varepsilon$  since  $\zeta \in (0, 1)$ .

The following theorem gives the convergence result of the SQH algorithm for solving (11)

**Theorem 4.1.** *Let  $(f^k, u^k)$  and  $(f^{k+1}, u^{k+1})$  be generated by the SQH method (algorithm 1) applied to (11), with  $u^{k+1}, u^k \in U_{ad}$ . Then for the current value of  $\varepsilon > 0$  chosen by algorithm 1, the following inequality holds:*

$$(26) \quad J(f^{k+1}, u^{k+1}) - J(f^k, u^k) = -\varepsilon \|u^{k+1} - u^k\|_{(L^2[0,T])^3}^2.$$

*In particular, this implies  $J(f^{k+1}, u^{k+1}) - J(f^k, u^k) = -\mu \tau$  for  $\varepsilon = \mu$  and  $\tau = \|u^{k+1} - u^k\|_{(L^2[0,T])^3}^2$ .*

**Algorithm 1** Sequential Quadratic Hamiltonian Method for Resolving Optimal Control Maps

---

(1) Input: initial approximation  $u^0$ , maximum number of iterations  $k_{max}$ , tolerance  $\kappa > 0$ ,  $\varepsilon > 0$ ,  $\lambda > 1$ ,  $\mu > 0$ , and  $\zeta \in (0, 1)$ .

(2) Set  $k = 0$  and compute the solution  $f^0$  to the FP equation (FP) with control  $u = u^0$ .

(3) Perform the following iteration.

**repeat**

(i) Compute the solution  $q^k$  to the adjoint equation (ADJ) with  $f = f^k$  and  $u = u^k$ .

(ii) Compute  $u^{k+1}$  satisfying the following for a.e.  $t \in [0, T]$  :

$$H_\varepsilon \left( t, f^k(\cdot, t), q^k(\cdot, t), u^k(t), u^{k+1}(t) \right) = \min_{w \in R_U} H_\varepsilon \left( t, f^k(\cdot, t), q^k(\cdot, t), u^k(t), w \right)$$

(iii) Compute the solution  $f^{k+1}$  to the Fokker-Planck equation (FP) with control  $u = u^{k+1}$ .

(iv) Compute  $\tau = \|u^{k+1} - u^k\|_{(L^2[0,T])^3}^2$ .

(v) **if**:  $\{J(f^{k+1}, u^{k+1}) - J(f^k, u^k) > -\mu \tau\}$  then set  $\varepsilon \leftarrow \lambda \varepsilon$  and return to step (ii),  
**else if**:  $\{J(f^{k+1}, u^{k+1}) - J(f^k, u^k) \leq -\mu \tau\}$ , then set  $\varepsilon \leftarrow \zeta \varepsilon$  and continue.

(vi) Set  $k \leftarrow k + 1$ .

**until**  $k = k_{max}$  or  $\tau < \kappa$

---

*Proof.* In step (iii) of algorithm 1, for almost all  $t \in [0, T]$ , we have:

$$H_\varepsilon(t, f^k, q^k, u^k, u^{k+1}) \leq H_\varepsilon(t, f^k, q^k, u^k, w),$$

for all  $w \in R_U$ . This implies

$$H_\varepsilon(t, f^k, q^k, u^k, u^{k+1}) \leq H_\varepsilon(t, f^k, q^k, u^k, u^k) = H(t, f^k, q^k, u^k).$$

Thus, we obtain the inequality

$$H(t, f^k, q^k, u^{k+1}) + \epsilon \|u^{k+1} - u^k\|_2^2 \leq H(t, f^k, q^k, u^k),$$

and applying lemma 3.2, we have

$$\begin{aligned} J(f^{k+1}, u^{k+1}) - J(f^k, u^k) &= \int_0^T \left( H(t, f^k, q^k, u^{k+1}) - H(t, f^k, q^k, u^k) \right) dt \\ &\leq -\epsilon \|u^{k+1} - u^k\|_{(L^2[0,T])^3}^2, \end{aligned}$$

as desired.  $\square$

As a consequence of theorem 4.1, we have the following result guaranteeing that algorithm 1 will terminate.

**Theorem 4.2.** *If  $\varepsilon = \mu$  is chosen in algorithm 1 then*

- (a) *the sequence  $\{J(f^k, u^k)\}$  is decreasing and thus converges to some  $J^* \geq \inf_{f,u} J(f, u)$ ,*
- (b)  $\lim_{k \rightarrow \infty} \|u^{k+1} - u^k\|_{(L^2[0,T])^3} = 0$

*Proof.* Statement (a) follows directly from (26), and convergence follows since the sequence is decreasing and bounded below.

For statement (b), we rearrange (26) to read

$$\|u^{k+1} - u^k\|_{(L^2[0,T])^3} \leq \frac{1}{\mu} (J(f^k, u^k) - J(f^{k+1}, u^{k+1}))$$

whereupon we have the telescoping partial sum

$$0 \leq \sum_{k=0}^K \|u^{k+1} - u^k\|_{(L^2[0,T])^3} \leq \frac{1}{\mu} (J(f^0, u^0) - J(f^{K+1}, u^{K+1})).$$

Taking  $K \rightarrow \infty$  shows that the infinite series converges, so the summands must tend to zero, achieving (b).  $\square$

In particular, this shows that in algorithm 1, if one chooses  $\varepsilon = \mu$ , then for any tolerance  $\kappa > 0$ , the convergence criterion  $\tau < \kappa$  will be reached in finitely many steps. Further, the Lipschitz continuity of the control-to-state map derived in lemma 3.1 shows that  $\|f^{k+1} - f^k\|_{L^2(Q)}$  (and indeed stronger norms) will also tend to zero.

## 5. RESULTS

In this section, we present the results of our FP control framework (11) simulated using the SQH algorithm. In all simulations we set  $b = \delta = 0.01$ . Having done so, solutions  $S, I, R$  of the deterministic model (1) will satisfy  $S + I + R \rightarrow 1$  as  $t \rightarrow \infty$ . Accordingly, if we choose  $S_0 \in [0, 1]$  and  $I_0$  positive but close to zero, we empirically observe that  $S(t), I(t) \in [0, 1]$  for all  $t$ . Because of this, we choose the spatial domain of the FP equation (6) to be  $[0, 1] \times [0, 1]$ . With infection rate  $\beta_3$  and recovery rate  $\gamma = 1$ , the disease dynamics have more-or-less entirely played out by time  $T = 10$  (see figure 2, top). The values of the upper bounds of the controls  $\alpha, \eta$  and  $v$  are set to  $\alpha_{\max} = 0.85$ ,  $\eta_{\max} = 0.25\gamma$  and  $v_{\max} = 0.1$ , respectively denoting that the maximum decrease in infection rate due to non-pharmaceutical intervention is 85%, the maximum achievable increase in recovery rate due to treatment efforts is 25%, and the maximum vaccination rate is 10% of the population per unit time. For initial distribution of  $(S_0, I_0)$ , we consider a normal distribution centered at  $(0.99, 0.01)$  with variance 0.025 (we then multiply the distribution function by the indicator function of  $[0, 1] \times [0, 1]$  and normalize in  $L^1$ ). The diffusion coefficients are chosen to in the spirit of [26, 38]:

$$\sigma_S = -\sigma_I = \sqrt{0.02}(1 - \alpha)SI$$

which is meant to express uncertainty in the infection rate. We use a mixed  $L^1/L^2$  control cost

$$\ell(u) = \beta_1 \|u\|_1 + \frac{\beta_2}{2} \|u\|_2^2$$

where  $\beta_1, \beta_2$  are constant. For our simulations we take  $\beta_1 = 0.2, \beta_2 = 0.1$ , though any nonnegative choices are acceptable. Henceforth we fix all of these parameters. We note that these are synthetic choices, chosen to demonstrate different aspects of the model and not to represent any particular epidemic in any particular region.

The initial guesses for the controls in the SQH algorithm are all set to 0. We discretize the spatial domain into 41 equally spaced points in each direction while the temporal grid consists of 81 equally spaced points. The hyperparameters for the SQH algorithm are set at  $\mu = 10^{-9}, \zeta = 0.9, \lambda = 1.1, \kappa = 10^{-3}$  and  $\varepsilon = 1$ . The maximum iteration count is  $k_{\max} = 150$  though this is never reached in our examples.

Before solving any control problems, we include results of the simulation in the *uncontrolled* scenario (i.e.  $\alpha, \eta, v \equiv 0$ ) for comparison. These results are seen in figure 2, where the top plots contain the deterministic disease dynamics following (1) starting from  $(S_0, I_0) = (0.99, 0.01)$ , and the bottom plots give snapshots of the solution  $f(x, t)$  of the Fokker-Planck equation (6) in the form

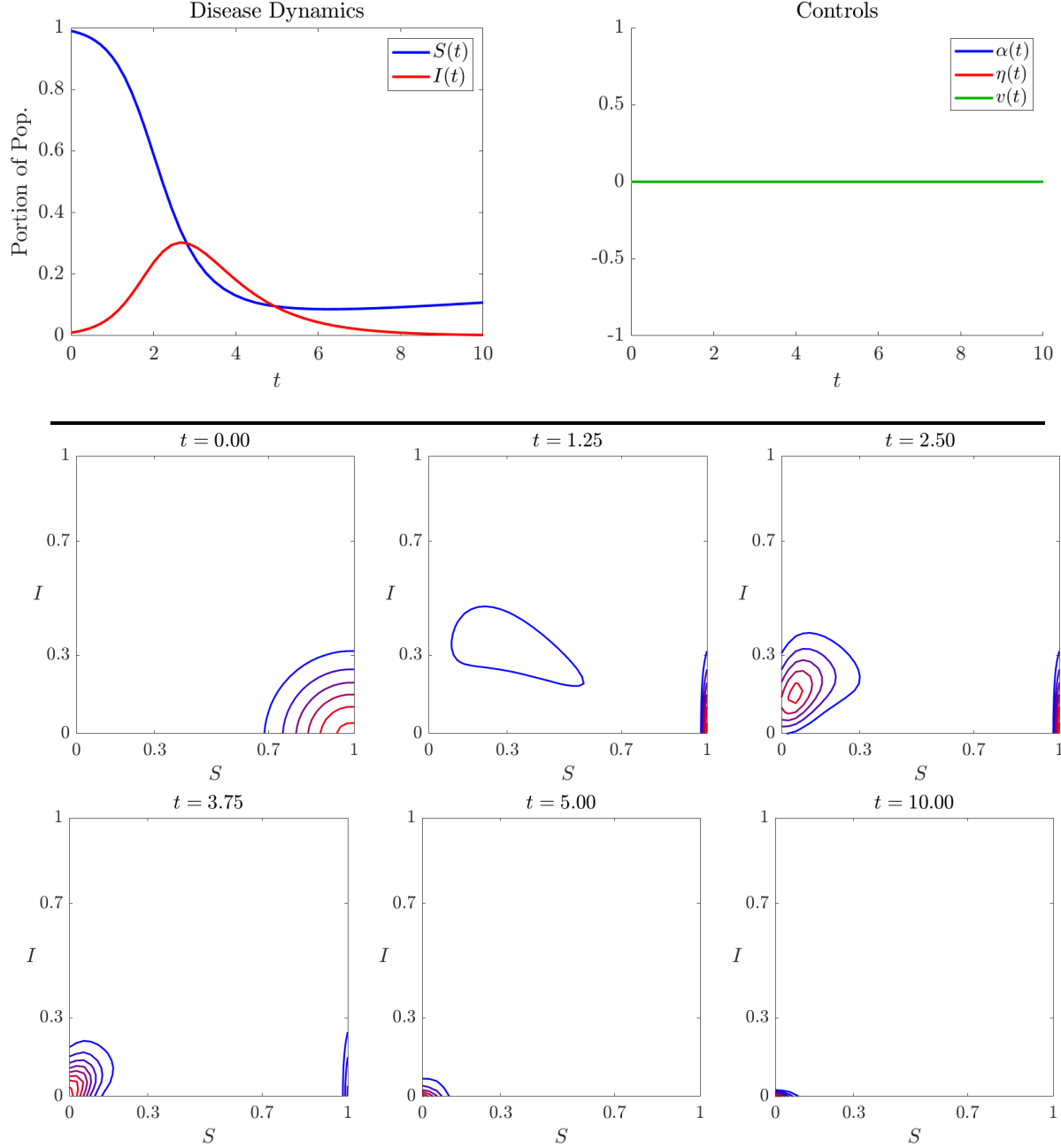


**Figure 2.** The dynamics corresponding to our choice of parameters in the *uncontrolled* case (i.e.  $\alpha, \eta, v \equiv 0$ ). Top: the deterministic disease dynamics governed by (1). Bottom: snapshots of the solution  $f(x, t)$  of the Fokker-Planck equation (6) in the form of contour plots with higher values in red and lower values in blue.

of contour plots where red contours represent higher values and blue contours represent lower values. The dynamics show a peak infection of roughly  $I = 0.3$  occurring at roughly  $t = 3$ . Referring to the distribution, we note that by time  $t = 5$  (and certainly by time  $t = 10$ ), essentially all the mass is centered near  $(S, I) = (0, 0)$ , meaning that the infection has run its course, and a vast majority of the population is in the recovered class. There are some interesting artifacts in the distribution function toward the lower right hand corner of the plots when  $t = 1.25, 2.50, 3.75$  which seem to

indicate that there is a nonzero chance that the susceptible population remains prominent until those times. This could possibly be explained by the observations of Bertozzi et al. [5] regarding the relationship between the time scale for the disease and the initial infected population. In essence, they conclude that for simple compartmental models lowering the initial infection size  $I_0$  will not affect the total infection size, but simply delay the onset of the wave of infections. The possibility of the susceptible population remaining large for such a long time could then be explained by the fact that our initial distribution allows for  $I_0$  values that are arbitrarily small.

Beyond this, we include three simulated scenarios involving optimal control. In each scenario, we choose different forms of the running cost  $G(x, t)$  and terminal cost  $K(x)$  from (11), corresponding to different concerns which a policy-maker may have. We recall that we are using variables  $x = (x_1, x_2) = (S, I)$  here.

**Scenario 1.** In this scenario, we take  $G(x, t) = 1.5I$  and  $K(x) \equiv 0$ , meaning there is no terminal cost and running cost is assessed purely based on the total number of infections (i.e. distribution functions  $f(x, t)$  are penalized when they have more mass located in regions where  $I$  is higher). Results of this simulation are contained in figure 3. In this case, the optimal control strategy is to implement maximum level of treatment efforts ( $\eta(t)$ ) in the early stages of disease spread, and then supplement this with some use of NPIs ( $\alpha(t)$ ) and vaccination ( $v(t)$ ) when the infections near their peak. The net effect of this is to significantly slow down disease spread, as seen in the bottom panels which display the evolution of the distribution function  $f(x, t)$  of possible states. Comparing the snapshots in figure 3 with the corresponding snapshots for the uncontrolled simulation in figure 2, we see that while the result at  $t = 10$  is roughly the same, the mass in the controlled case travels more slowly from right to left, and is more concentrated on regions with higher  $S$  and/or lower  $I$  throughout (as can be seen at  $t = 1.25, 2.50, 3.75, 5.00$ ).

**Scenario 2.** In this scenario, we still take terminal cost  $K(x) \equiv 0$ , but now choose running cost  $G(x, t) = 1_{\{I \geq 0.15\}}(x)$  to be the indicator function of the set  $\{I \geq 0.15\}$ ; that is,

$$G(x, t) = \begin{cases} 1, & I \geq 0.15, \\ 0, & I < 0.15. \end{cases}$$

We use this to model something like a hospital capacity constraint, wherein no cost is assessed for infections until they reach a certain threshold beyond which hospitals are over-burdened. This is chosen to mirror some rhetoric from the early days of the COVID19 pandemic, where policy-makers expressed concern over the excess burden to healthcare infrastructure and emphasized the need to “flatten the curve.” The results in figure 4 demonstrate that the optimal controls for this cost functional very effectively accomplish this goal. In the plots, we have included the line  $I = 0.15$  representing this threshold. Here the optimal control strategy is similar in the initial stages of the epidemic with maximal treatment efforts ( $\eta(t)$ ). It appears that in this initial stage, it is infeasible to keep all the mass for  $f(x, t)$  in the region  $\{I < 0.15\}$ . However, subsequently, the optimal strategy involves maximal employment of vaccination ( $v(t)$ ) and strong use of NPIs ( $\alpha(t)$ ) to quickly drive the majority of the mass for  $f(x, t)$  under the line  $I = 0.15$ . This is seen in the snapshots at times  $t = 2.50, 3.75, 5.00$  where the contours have been significantly flattened when compared with Scenario 1. Likewise, the dynamics in the top left of figure 4 exhibit precisely this “flattening the curve” behavior, wherein the epidemic is prolonged, but the peak of infections is much smaller than in Scenario 1 or in the uncontrolled case.

**Scenario 3.** Here we choose running cost  $G(x, t) \equiv 0$  and terminal cost  $K(x) = -\max(S - 0.3, 0)$ , and we assume that vaccination is unavailable so that  $v_{\max} = 0$ . Here, with  $K(x)$  negative, this is more akin to a profit that one can achieve by keeping the susceptible population at the end

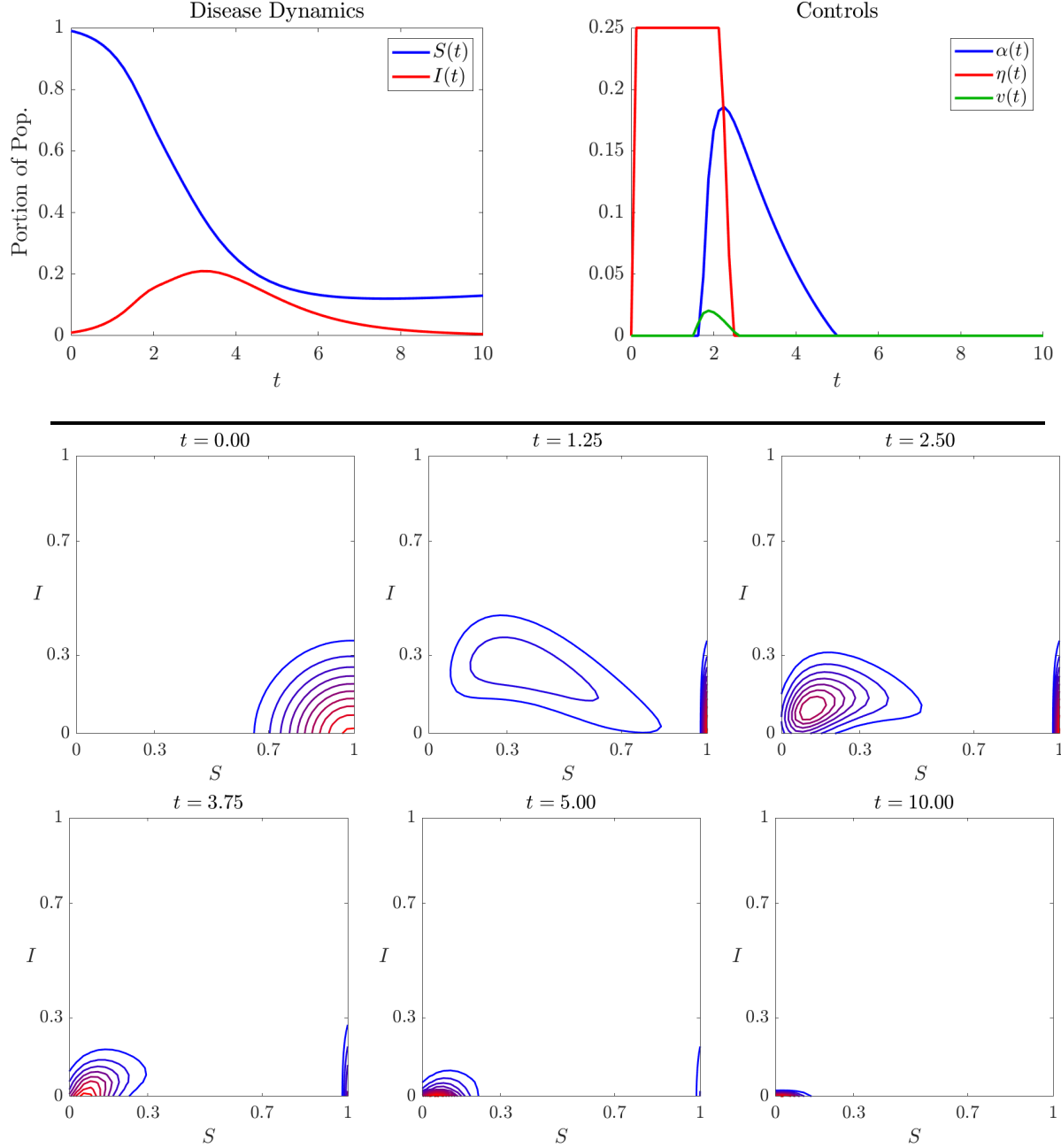


**Figure 3.** Scenario 1:  $G(x, t) = x_2 = I$ ,  $K(x) \equiv 0$ . In this scenario, the optimal control employs the maximal level of treatment efforts ( $\eta(t)$ ) in the initial stage of infections, and as infections near their peak, these efforts are supplemented with modest use of NPIs ( $\alpha(t)$ ) and vaccination ( $v(t)$ ).

time above the threshold 0.3. This scenario is meant to model the early stages of an epidemic wherein vaccines are not yet available, and the policy-maker would like to maintain a high level of susceptible population until the time that they are. The results are in figure 5. In this case, the only control that has meaningful effect is the NPIs ( $\alpha(t)$ ). These are employed at their maximal strength at the outset, and then taper off but continue to be employed at a steady rate throughout the course of the epidemic. This will significantly stunt disease spread, whereupon treatment efforts

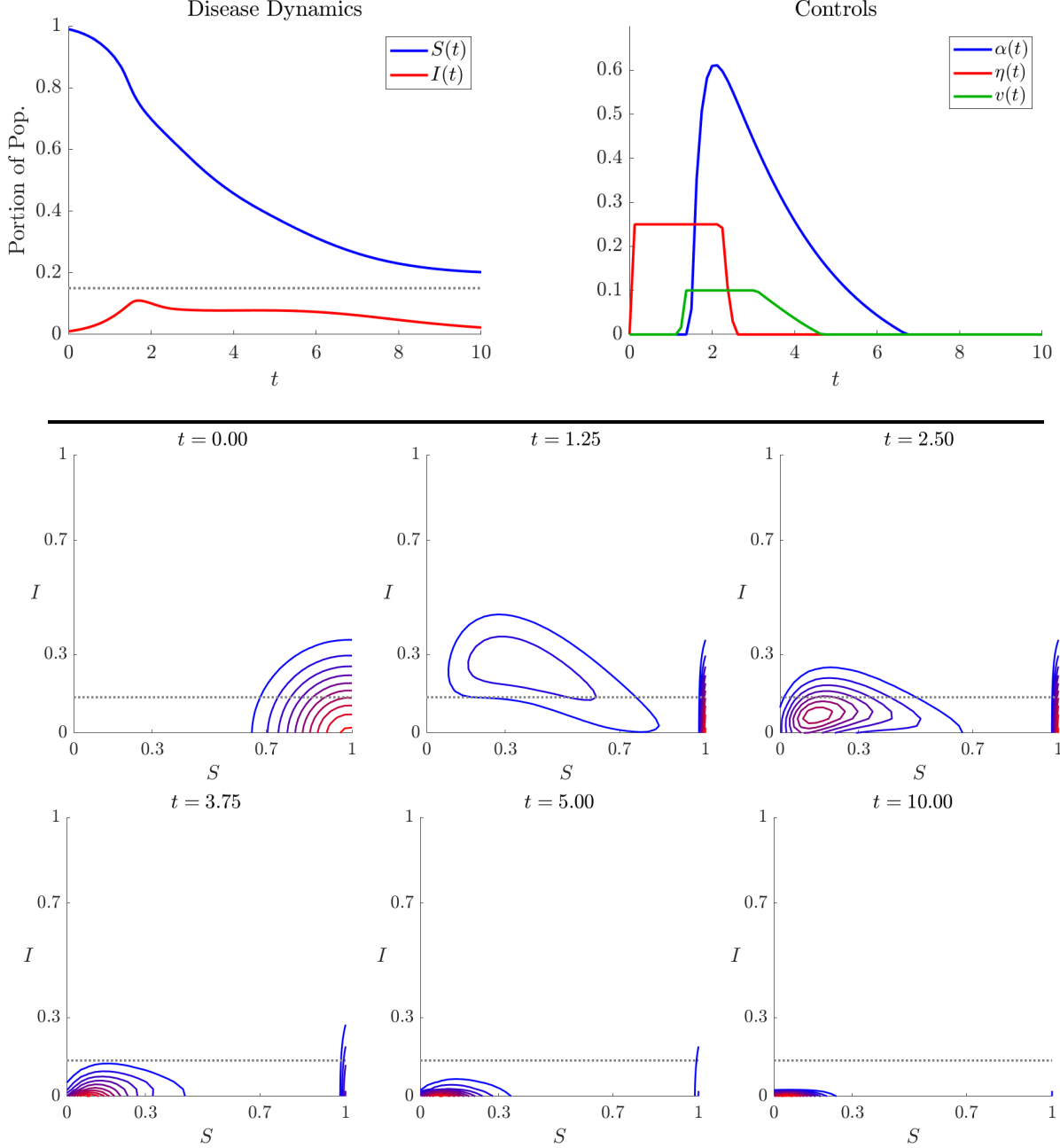


**Figure 4.** Scenario 2:  $G(x,t) = 1_{\{I \geq 0.15\}}(x)$ , the indicator function of the set  $\{I \geq 0.15\}$ ,  $K(x) \equiv 0$ . Here 0.15 is imagined to be the infection threshold past which the healthcare system would be overburdened. In this scenario, the optimal control uses the maximal level of treatment efforts ( $\eta(t)$ ) in the initial stage of infections, the maximum level of vaccination ( $v(t)$ ) during the peak infections, and a substantially stronger employment of NPIs ( $\alpha(t)$ ) than in Scenario 1. This has the effect of pushing the bulk of the mass for the distribution  $f(x,t)$  below the line  $I = 0.15$  (grey dotted line) much more quickly than in Scenario 1. With these controls, the dynamics (top left) exhibit a more prolonged but flattened epidemic.

$(\eta(t))$  are superfluous since there are essentially no new infected individuals who would benefit from an increased recovery rate. We have plotted the threshold  $S = 0.3$  as green dotted lines in the plot of the dynamics and the snapshots of the density function  $f(x,t)$ . Here the effect of the controls is

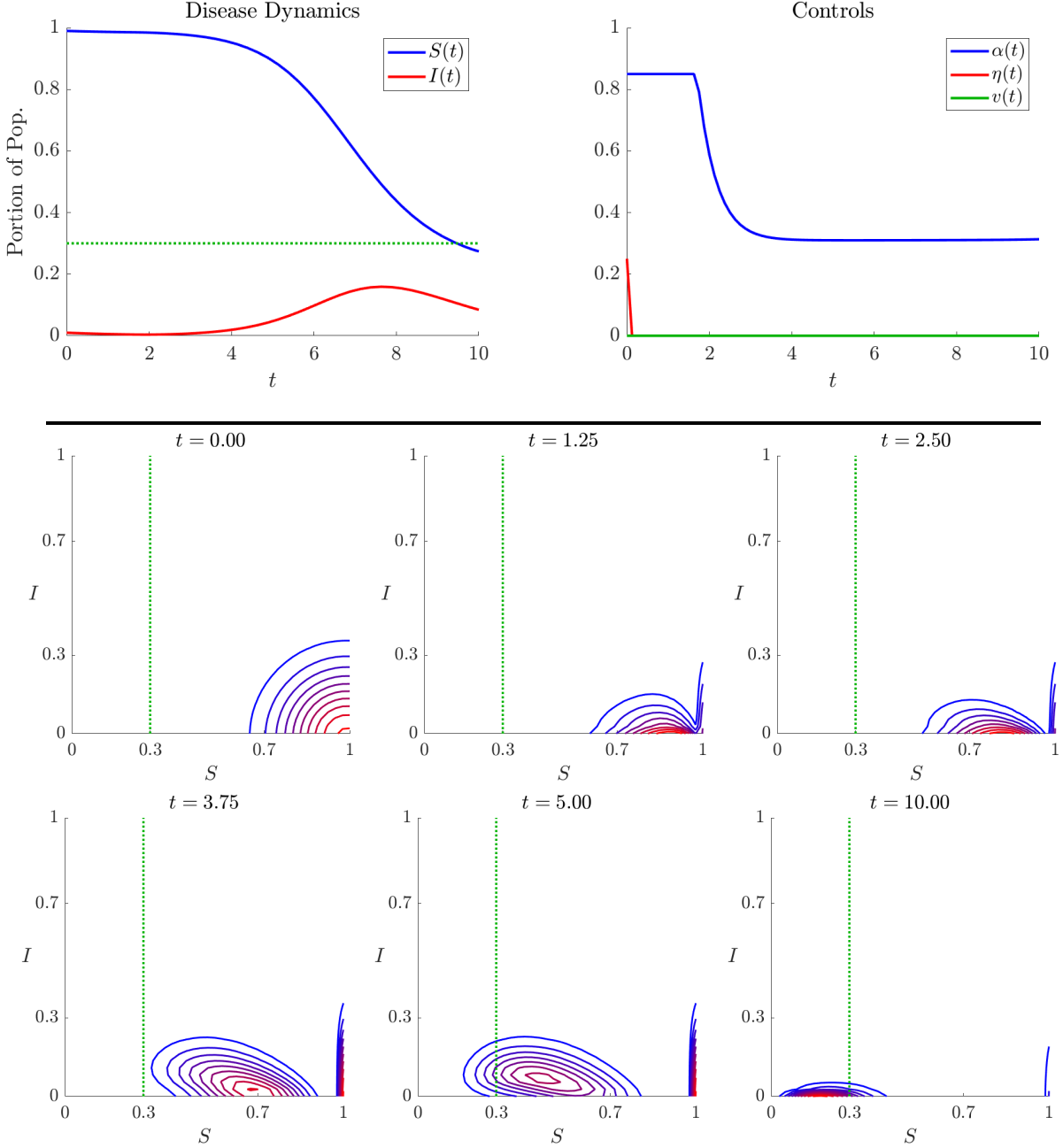


**Figure 5.** Scenario 3:  $G(x, t) \equiv 0$ ,  $K(x) = -\max(S - 0.3, 0)$ ,  $v(t) \equiv 0$ . Here we simulate a scenario where vaccination is unavailable, and the only goal is to maintain a sufficiently large susceptible population by the end time. In this case, the optimal strategy entails very strong use of NPIs ( $\alpha(t)$ ), and little to no use of treatment efforts ( $\eta(t)$ ). The result is that the mass of the distribution function  $f(x, t)$  moves much more slowly toward states with lower  $S$  value, and ends with a nontrivial portion of the mass above the threshold  $S = 0.3$  (green dotted line). In this case, the particular dynamics land below this threshold at time  $t = 10$  (top left).

to significantly slow the drift of the mass of  $f(x, t)$  toward states with lower  $S$ , such that, by  $t = 10$ , there is still a nontrivial amount of mass which lies in the region  $S \geq 0.3$ . That said, less than half the mass lies in this region, meaning that one is likely to end with  $S < 0.3$ , as is seen in the dynamics in the top left of figure 5. This is a key difference between the Fokker-Planck framework

for control and the direct control of the ODE system (1). In this case, one could say that the controls failed for this individual trajectory of the dynamics, in the sense that it lands below the threshold  $S = 0.3$  at time  $t = 10$ . However, cost is not being assessed for individual trajectories but rather for the distribution of possible trajectories. Here it seems that it was optimal to save some cost by arriving at a distribution wherein some small portion of the trajectories will indeed land above the threshold  $S = 0.3$ , while many will not.

## 6. CONCLUSIONS & FUTURE WORK

In this manuscript, we have presented a framework for control of a stochastic compartmental model in mathematical epidemiology. The strategy entails controlling the associated Fokker-Planck equation, rather than controlling individual trajectories of the stochastic system. We formulate an optimal control problem involving a relatively general cost functional, prove existence of optimal controls, and derive first order optimality conditions which characterize the optimal controls. We describe the application of the sequential quadratic Hamiltonian method [11] to our problem, and numerically resolve the optimal control maps for three different scenarios involving different policy-maker preferences.

While the model presented is, admittedly, quite simple, this serves as a proof of concept that the Fokker-Planck control framework can be meaningfully applied to control of stochastic compartmental models for epidemiology, while allowing for uncertainty in initial data. As an immediate avenue of future work, the authors would like to apply a similar framework to more realistic models involving more heterogeneity, and in particular, to models like those developed by the first author which incorporate human behavior [8, 36, 38]. The barrier to doing so is that these models involves several additional compartments, and each compartment in the model becomes an additional “spatial” dimension in the Fokker-Planck equation, meaning that grid-based numerical methods will be infeasible. Numerically solving high-dimensional PDE is an area of active research with popular approaches including tensor decomposition [18, 19, 51] and pseudo-spectral methods [2, 15, 49, 53]. Development of similar schemes in the context of the Fokker-Planck equation would afford one the opportunity to apply our framework to a much broader class of epidemic models and thus greatly increase in the realism.

## ACKNOWLEDGMENTS

CP would like to thank Marcelo Bongarti for helpful discussions regarding the theoretical aspects of the optimal control problem. The work of SR was supported by the National Science Foundation grant numbers 2309491 and 2230790.

## REFERENCES

- [1] M. ANNUNZIATO AND A. BORZÌ, *A Fokker-Planck control framework for stochastic systems*, EMS Surveys in Mathematical Sciences, 5 (2018), pp. 65–98.
- [2] H. ANTIL, P. DONDL, AND L. STRIET, *Approximation of integral fractional laplacian and fractional PDEs via sinc-basis*, SIAM Journal on Scientific Computing, 43 (2021), pp. A2897–A2922.
- [3] H. ANTIL AND D. LEYKEKHMAN, *A brief introduction to PDE-constrained optimization*, Frontiers in PDE-constrained optimization, 163 (2018), p. 434.
- [4] T. BARBU, C. MOROŞANU, AND S.-D. PAVĂL, *A Fokker-Planck model for optical flow estimation and image registration*, Mathematics, 13 (2025), p. 2807.
- [5] A. L. BERTOZZI, E. FRANCO, G. MOHLER, M. B. SHORT, AND D. SLEDGE, *The challenges of modeling and forecasting the spread of COVID-19*, Proceedings of the National Academy of Sciences, 117 (2020), pp. 16732–16738.
- [6] M. H. A. BISWAS, L. T. PAIVA, M. D. R. DE PINHO, ET AL., *A SEIR model for control of infectious diseases with constraints*, Mathematical Biosciences and Engineering, 11 (2014), pp. 761–784.
- [7] L. BOLZONI, E. BONACINI, C. SORESINA, AND M. GROPPYI, *Time-optimal control strategies in SIR epidemic models*, Mathematical biosciences, 292 (2017), pp. 86–96.

- [8] M. BONGARTI, L. D. GALVAN, L. HATCHER, M. R. LINDSTROM, C. PARKINSON, C. WANG, AND A. L. BERTOZZI, *Alternative SIAR models for infectious diseases and applications in the study of non-compliance*, Mathematical Models and Methods in Applied Sciences, 32 (2022), pp. 1987–2015.
- [9] M. BONGARTI, C. PARKINSON, AND W. WANG, *Optimal control of a reaction-diffusion epidemic model with non-compliance*, European Journal of Applied Mathematics, (2025), pp. 1–26.
- [10] A. BORZÌ, *The Fokker-Planck framework in the modeling of pedestrians' motion*, in Crowd Dynamics, Volume 2: Theory, Models, and Applications, Springer, 2020, pp. 111–131.
- [11] ———, *The Sequential Quadratic Hamiltonian Method: Solving Optimal Control Problems*, Chapman and Hall/CRC, 2023.
- [12] T. BREITENBACH AND A. BORZÌ, *The Pontryagin maximum principle for solving Fokker-Planck optimal control problems*, Computational Optimization and Applications, 76 (2020), pp. 499–533.
- [13] H. BRÉZIS, *Functional analysis, Sobolev spaces and partial differential equations*, vol. 2, Springer, 2011.
- [14] R. BROCKETT, *Notes on the control of the Liouville equation*, in Control of Partial Differential Equations: Cetraro, Italy 2010, Editors: Piermarco Cannarsa, Jean-Michel Coron, Springer, 2012, pp. 101–129.
- [15] J. BURKARDT, Y. WU, AND Y. ZHANG, *A unified meshfree pseudospectral method for solving both classical and fractional pdes*, SIAM Journal on Scientific Computing, 43 (2021), pp. A1389–A1411.
- [16] L. CHANG, W. GONG, Z. JIN, AND G.-Q. SUN, *Sparse optimal control of pattern formations for an SIR reaction-diffusion epidemic model*, SIAM Journal on Applied Mathematics, 82 (2022), pp. 1764–1790.
- [17] J. C. DAGHER AND C. PARKINSON, *Optimal lockdowns under constraints*, Economic Inquiry, 63 (2025), pp. 523–544.
- [18] A. DEKTOR AND D. VENTURI, *Dynamic tensor approximation of high-dimensional nonlinear PDEs*, Journal of Computational Physics, 437 (2021), p. 110295.
- [19] S. DOLGOV, D. KALISE, AND K. K. KUNISCH, *Tensor decomposition methods for high-dimensional Hamilton-Jacobi-Bellman equations*, SIAM Journal on Scientific Computing, 43 (2021), pp. A1625–A1650.
- [20] H. EDDUWEH AND S. ROY, *A Liouville optimal control framework in prostate cancer*, Applied Mathematical Modelling, 134 (2024), pp. 417–433.
- [21] L. C. EVANS, *Partial differential equations*, vol. 19, American mathematical society, 2022.
- [22] W. H. FLEMING AND R. W. RISHEL, *Deterministic and stochastic optimal control*, vol. 1, Springer Science & Business Media, 2012.
- [23] J. A. GONDIM AND L. MACHADO, *Optimal quarantine strategies for the COVID-19 pandemic in a population with a discrete age structure*, Chaos, Solitons & Fractals, 140 (2020), p. 110166.
- [24] A. GRAY, D. GREENHALGH, L. HU, X. MAO, AND J. PAN, *A stochastic differential equation SIS epidemic model*, SIAM Journal on Applied Mathematics, 71 (2011), pp. 876–902.
- [25] J. JANG, H.-D. KWON, AND J. LEE, *Optimal control problem of an SIR reaction-diffusion model with inequality constraints*, Mathematics and Computers in Simulation, 171 (2020), pp. 136–151.
- [26] C. JI, D. JIANG, AND N. SHI, *The behavior of an SIR epidemic model with stochastic perturbation*, Stoch. Anal. Appl., 30 (2012), pp. 755–773.
- [27] D. JIANG, J. YU, C. JI, AND N. SHI, *Asymptotic behavior of global positive solution to a stochastic SIR model*, Mathematical and Computer Modelling, 54 (2011), pp. 221–232.
- [28] H. R. JOSHI, S. LENHART, S. HOTA, AND F. AGUSTO, *Optimal control of an SIR model with changing behavior through an education campaign*, Electronic Journal of Differential Equations, 2015 (2015), pp. 1–14.
- [29] W. O. KERMACK AND A. G. MCKENDRICK, *A contribution to the mathematical theory of epidemics*, Proceedings of the royal society of london. Series A, Containing papers of a mathematical and physical character, 115 (1927), pp. 700–721.
- [30] A. A. KHAN, S. ULLAH, AND R. AMIN, *Optimal control analysis of COVID-19 vaccine epidemic model: a case study*, The European Physical Journal Plus, 137 (2022), pp. 1–25.
- [31] O. A. LADYZHENSKAJA, V. A. SOLONNIKOV, AND N. N. URAL'TSEVA, *Linear and quasi-linear equations of parabolic type*, vol. 23, American Mathematical Soc., 1968.
- [32] J. C. LEMAITRE, D. PASETTO, M. ZANON, E. BERTUZZO, L. MARI, S. MICCOLI, R. CASAGRANDI, M. GATTO, AND A. RINALDO, *Optimal control of the spatial allocation of COVID-19 vaccines: Italy as a case study*, PLoS computational biology, 18 (2022), p. e1010237.
- [33] S. LENHART AND J. T. WORKMAN, *Optimal control applied to biological models*, Chapman and Hall/CRC, 2007.
- [34] G. LEONI, *A first course in Sobolev spaces*, American Mathematical Soc., 2017.
- [35] A. MANZONI, A. QUATERONI, AND S. SALSA, *Optimal control of partial differential equations*, Springer, 2021.
- [36] C. NGO, C. PARKINSON, AND W. WANG, *Optimal control of an SIR model with noncompliance as a social contagion*, arXiv preprint arXiv:2509.09075, (2025).
- [37] F. PARINO, L. ZINO, AND A. RIZZO, *Optimal control of endemic epidemic diseases with behavioral response*, IEEE open journal of control systems, (2024).

- [38] C. PARKINSON AND W. WANG, *A compartmental model for epidemiology with human behavior and stochastic effects*, Mathematical Biosciences, 392 (2026), p. 109588.
- [39] A. RAJPUT, M. SAJID, TANVI, C. SHEKHAR, AND R. AGGARWAL, *Optimal control strategies on COVID-19 infection to bolster the efficacy of vaccination in India*, Scientific Reports, 11 (2021), p. 20124.
- [40] H. RISKEN, *Fokker-Planck equation: methods of solution and applications*, Springer Berlin, Heidelberg, 1996.
- [41] S. ROY, *A sparsity-based Fokker-Planck optimal control framework for modeling traffic flows*, in AIP Conference Proceedings, vol. 2302, 2020, p. 110007.
- [42] S. ROY, M. ANNUNZIATO, AND A. BORZÌ, *A Fokker-Planck feedback control-constrained approach for modelling crowd motion*, Journal of Computational and Theoretical Transport, 45 (2016), pp. 442–458.
- [43] S. ROY, M. ANNUNZIATO, A. BORZÌ, AND C. KLINGENBERG, *A Fokker-Planck approach to control collective motion*, Computational Optimization and Applications, 69 (2018), pp. 423–459.
- [44] S. ROY AND A. BORZÌ, *Numerical approximation of kinetic Fokker-Planck equations with specular reflection boundary conditions*, Journal of Computational Physics, 503 (2024), p. 112841.
- [45] S. ROY, Z. PAN, AND S. PAL, *A Fokker-Planck feedback control framework for optimal personalized therapies in colon cancer-induced angiogenesis*, Journal of mathematical biology, 84 (2022), p. 23.
- [46] W. RUDIN, *Real and complex analysis*, McGraw-Hill, Inc., 1987.
- [47] C. SCHNEIDER AND W. ALT, *Regularization of linear-quadratic control problems with  $l_1$ -control cost*, in IFIP Conference on System Modeling and Optimization, Springer, 2013, pp. 296–305.
- [48] E. SHAKERI, G. LATIF-SHABGAHI, AND A. E. ABHARIAN, *Predictive drug dosage control through a Fokker-Planck observer*, Computational and Applied Mathematics, 37 (2018), pp. 3813–3831.
- [49] Z. SHAO, K. PIEPER, AND X. TIAN, *Solving nonlinear PDEs with sparse radial basis function networks*, arXiv preprint arXiv:2505.07765, (2025).
- [50] C. J. SILVA, C. CRUZ, D. F. TORRES, A. P. MUNUZURI, A. CARBALLOSA, I. AREA, J. J. NIETO, R. FONSECA-PINTO, R. PASSADOURO, E. S. D. SANTOS, ET AL., *Optimal control of the COVID-19 pandemic: controlled sanitary deconfinement in Portugal*, Scientific reports, 11 (2021), p. 3451.
- [51] X. TANG, N. SHENG, AND L. YING, *Solving high-dimensional Hamilton-Jacobi-Bellman equation with functional hierarchical tensor*, arXiv preprint arXiv:2408.04209, (2024).
- [52] T. TAO, *An introduction to measure theory*, vol. 126, American Mathematical Soc., 2011.
- [53] A. THOMANN AND A. BORZÌ, *Stability and accuracy of a pseudospectral scheme for the Wigner function equation*, Numerical Methods for Partial Differential Equations, 33 (2017), pp. 62–87.
- [54] E. TORNATORE, S. MARIA BUCCELLATO, AND P. VETRO, *Stability of a stochastic SIR system*, Physica A: Statistical Mechanics and its Applications, 354 (2005), pp. 111–126.
- [55] F. TRÖLTZSCH, *Optimal control of partial differential equations: theory, methods, and applications*, vol. 112, American Mathematical Soc., 2010.
- [56] G. VOSSEN AND H. MAURER, *On  $l_1$ -minimization in optimal control and applications to robotics*, Optimal Control Applications and Methods, 27 (2006), pp. 301–321.
- [57] A. WÄCHTER AND L. T. BIEGLER, *On the implementation of an interior-point filter line-search algorithm for large-scale nonlinear programming*, Mathematical programming, 106 (2006), pp. 25–57.
- [58] Z. WU, J. YIN, AND C. WANG, *Elliptic and parabolic equations*, World Scientific Publishing Company, 2006.
- [59] K. YAMAZAKI, *Global existence, uniqueness, and non-negativity of the solutions to stochastic partial differential equations of infectious diseases*, La Matematica, 3 (2024), pp. 994–1015.
- [60] J. YONG AND X. Y. ZHOU, *Stochastic controls: Hamiltonian systems and HJB equations*, vol. 43, Springer Science & Business Media, 1999.
- [61] O. ZAKARY, M. RACHIK, AND I. ELMOUKI, *On the analysis of a multi-regions discrete SIR epidemic model: an optimal control approach*, International Journal of Dynamics and Control, 5 (2017), pp. 917–930.
- [62] Y. ZHOU, W. ZHANG, AND S. YUAN, *Survival and stationary distribution of a SIR epidemic model with stochastic perturbations*, Applied Mathematics and Computation, 244 (2014), pp. 118–131.

Christian Parkinson, Department of Mathematics & Department of Computational Mathematics, Science and Engineering, Michigan State University, East Lansing, MI, USA; e-mail: [chparkin@msu.edu](mailto:chparkin@msu.edu)

Souvik Roy, Department of Mathematics, University of Texas at Arlington, Arlington, TX, USA; e-mail: [souvik.roy@uta.edu](mailto:souvik.roy@uta.edu)